



Characterization of winter PM_{2.5} source contributions and impacts of meteorological conditions and anthropogenic emission changes in the Sichuan Basin, 2002–2020

Yaohan Xian ^a, Yang Zhang ^{a,b,c,*}, Zhihong Liu ^{a,b,c}, Haofan Wang ^d, Tianxin Xiong ^a

^a College of Resources and Environment, Chengdu University of Information Technology, Chengdu 610225, China

^b Key Laboratory of Atmospheric Environment Simulation and Pollution Control at Chengdu University of Information Technology of Sichuan Province, Chengdu 610225, China

^c Chengdu Plain Urban Meteorology and Environment Observation and Research Station of Sichuan Province, Chengdu University of Information Technology, Chengdu 610225, China

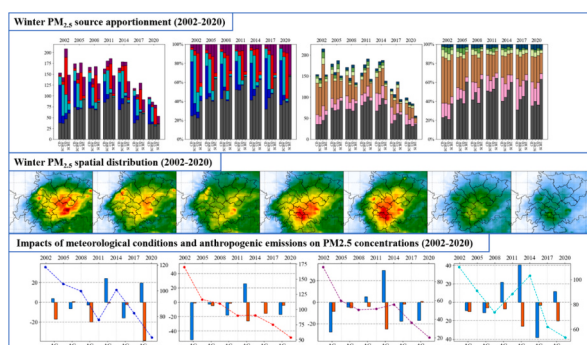
^d School of Atmospheric Sciences, Sun Yat-sen University, and Southern Marine Science and Engineering Guangdong Laboratory (Zhuhai), Zhuhai 519082, China



HIGHLIGHTS

- Sichuan basin's winter PM_{2.5} dropped from 300 to 120 µg/m³ over 20 years.
- East basin records highest winter PM_{2.5} decrease from 148 to 54 µg/m³ over years.
- Residential PM_{2.5} falls from 46 % to 27 % ultimately matching industrial PM_{2.5}.
- Meteorological conditions can change basin's annual PM_{2.5} by 20–40 µg/m³.

GRAPHICAL ABSTRACT



ARTICLE INFO

Editor: Hai Guo

Keywords:

PM_{2.5}
Meteorological variability
Source apportionment
Sichuan Basin

ABSTRACT

In this study, the Weather Research and Forecasting (WRF) model and Community Multiscale Air Quality–Integrated Source Apportionment Method (CMAQ–ISAM) were utilized, which were integrated with the Multiresolution Emission Inventory for China (MEIC) emission inventory, to simulate winter PM_{2.5} concentrations, regional transport, and changes in emission source contributions in the Sichuan basin (SCB) from 2002 to 2020, considering variations in meteorological conditions and anthropogenic emissions. The results indicated a gradual decrease in the basin's winter average PM_{2.5} concentration from 300 µg/m³ to 120 µg/m³, with the most significant decrease occurring after 2014, reflecting the actual impact of China's air pollution control measures. Spatially, the main pollution area shifted from Chongqing to Chengdu and the western basin. The sources of PM_{2.5} at the eastern and western margins of the basin have remained stable and have been dominated by local emissions for many years, while the sources of PM_{2.5} in the central part of the basin have evolved from a multiregional co-influenced source during the early period to a high proportion of local emissions; except for boundary condition sources, residential sources were the main PM_{2.5} sources in the basin (approximately 29.70

* Corresponding author at: College of Resources and Environment, Chengdu University of Information Technology, Chengdu 610225, China.
E-mail address: zhangyang@cuit.edu.cn (Y. Zhang).

%), followed by industrial sources (approximately 14.11 %). Industrial sources exhibited higher contributions in Chengdu and Chongqing and gradually stabilized with residential sources over the years, while residential sources dominated in the eastern and western parts of the basin and exhibited a declining trend. Meteorological conditions exacerbated pollution in the whole basin from 2008 to 2014, especially in the west ($21\text{--}40 \mu\text{g}/\text{m}^3$). The eastern basin and Chongqing exhibited more years with alleviated meteorological pollution, including a $40+\mu\text{g}/\text{m}^3$ decrease in Chongqing from 2002 to 2005. Reduced anthropogenic emissions alleviated annual pollution levels, with a greater reduction ($> -20 \mu\text{g}/\text{m}^3$) after 2011 due to pollution control measures.

1. Introduction

$\text{PM}_{2.5}$ (particulate matter with aerodynamic diameters of $<2.5 \mu\text{m}$) is a complex mixture of elemental carbon, organic carbon, nitrate, ammonium, sulfate, and mineral dust formed by the physicochemical transformation of large amounts of gaseous precursors, i.e., sulfur dioxide (SO_2), nitrogen oxides (NO_x), and ammonia (NH_3) (He et al., 2001). It is one of the major air pollutants in China and is closely related to public and human health (Geng et al., 2021), global climate change (Bellouin et al., 2020), and the formation of pollution by regional haze (Tao et al., 2012). Since 2000, the gross domestic product (GDP) of China, the world's largest developing country, has increased by approximately seven times as a result of rapid economic development and the accelerating urbanization of its regions (Xu et al., 2020). However, emissions of air pollutants during the development process have subsequently increased dramatically and have been accompanied by severe environmental damage and deterioration of air quality (He et al., 2016; Xing et al., 2015). In response to severe and extensive air pollution, the Chinese government initiated policies that included controls on SO_2 during the 11th Five-Year Plan (2006–2010) and on both SO_2 and NO_x during the 12th Five-Year Plan (2011–2015) (Zheng et al., 2019). The National Air Pollution Prevention and Control Action Plan (NAPPAP) was launched in 2013 to implement more aggressive air pollution prevention and control measures. By 2017, $\text{PM}_{2.5}$ concentrations in major metropolitan areas were reduced by 25 % compared to those in 2013 (Cheng et al., 2019). While these measures have improved overall air quality in China, many cities have yet to meet the current National Ambient Air Quality Standards (NAAQS) (Tao et al., 2017).

The concentration and spatiotemporal distribution of $\text{PM}_{2.5}$ are influenced primarily by the chemical transformation of anthropogenic emissions, regional transport, and meteorological conditions (An et al., 2019; Gonzalez-Salazar et al., 2018; Liu and Wang, 2020). The interplay of various factors contributes to the complexity of regional air pollution issues, particularly in China's major urban clusters—including Beijing-Tianjin-Hebei (BTH), the Yangtze River Delta (YRD), the Pearl River Delta (PRD), the Sichuan Basin (SCB), and the Fenwei Plain (FWP)—where air pollution remains severe (Deng et al., 2022). To investigate air pollution, chemical transport models (CTMs) are primarily used to simulate atmospheric pollutant concentrations in major polluted areas, understand reaction processes, determine source apportionment, and determine regional transport contributions. This analysis of simulated typical pollution events and long-term progress in control enables the proposal of optimized management strategies (Li et al., 2021). Numerous studies have conducted characteristic analyses of pollutants in respective urban clusters using the Community Multiscale Air Quality (CMAQ) model, focusing on the resolution of emission sources and the variability of meteorological impacts. Feng et al. (2022) employed the Integrated Source Apportionment Method (ISAM) module with a priori/posteriori modeling to determine that the local contribution is greatest in the Yangtze River Delta under stable weather conditions, while unstable conditions increase the contribution from upwind areas. Lang et al. (2013) and Chang et al. (2019) utilized brute force methods and the ISAM, respectively, to simulate the transport characteristics of $\text{PM}_{2.5}$ in Beijing and concluded that regional transport from surrounding areas accounts for 42.2 % and 45.9 %, respectively, of Beijing's $\text{PM}_{2.5}$. Li et al. (2019) reported that in China's major polluted regions, the contributions

from regional transport to winter $\text{PM}_{2.5}$ from the NCP and YRD to the PRD and SCB (~5–25 %) are comparable to the contributions from regional transport and local emissions. In addition to pollution analyses that mainly focus on emission source characteristics, Shao et al. (2023) used the CMAQ model to simulate the characteristics of pollutants in major regions of China in 2013 and 2020 in terms of the impacts of emission sources and meteorological conditions on $\text{PM}_{2.5}$ and O_3 in each season; they concluded that, nationally, $\text{PM}_{2.5}$ decreased significantly (~40 %) during the study period and that the change in emission sources dictated the dominant annual average $\text{PM}_{2.5}$ decrease. Xu et al. (2020) employed the Weather Research and Forecasting–Community Multiscale Air Quality (WRF-CMAQ) model to simulate the annual average variations in $\text{PM}_{2.5}$ in major Chinese cities from 2000 to 2017, revealing a yearly decreasing trend in meteorological impacts with significant interprovincial variations.

The SCB is located in southwestern China; the basin has a total area of 260,000 km^2 , and the urban agglomeration includes the plains city of Chengdu and the mountainous city of Chongqing, which together form the Chengdu-Chongqing area, one of the most urbanized urban agglomerations in the western part of China (Gao et al., 2018). Influenced by the unique topography of the Tibetan and Yunnan-Guizhou Plateaus, the SCB experiences slow nocturnal temperature declines, small diurnal temperature ranges, and frequent air stagnation (Huang et al., 2017). The basin's distinctive atmospheric circulation patterns lead to frequent high-humidity fog events (Yu et al., 2015). Due to the dense population, urban development, and high pollution emissions in the Chengdu-Chongqing area, severe winter $\text{PM}_{2.5}$ pollution occurs (Niu et al., 2010). Since 2000, the basin has maintained high national annual average $\text{PM}_{2.5}$ concentrations (Liu et al., 2020). In 2015 and 2017, $\text{PM}_{2.5}$ pollution levels exceeded NAAQS standards, and extreme pollution events occurred in several cities within the basin (Ning et al., 2018). Recent research on pollution characteristics in the SCB has focused on its basin weather features, including analyses of pollution under regional weather systems using various statistical methods based on observational data and reanalysis material (Ning et al., 2018; Zhan et al., 2019). Studies on the chemophysical transformation of $\text{PM}_{2.5}$ components (Wang et al., 2018a) and wintertime urban air stagnation (Liao et al., 2018) in Chengdu and Chongqing, which are major cities in the SCB, have identified their distinctive urban climate and high anthropogenic emissions as key contributors to the region's atmospheric pollution. Qiao et al. conducted source apportionment and regional transport analysis of $\text{PM}_{2.5}$ within the basin for different years using the CMAQ-ISAM model (Qiao et al., 2019a; Qiao et al., 2019b; Qiao et al., 2021), while Wu et al. (2022) expanded upon these simulations by analyzing the impact of changes in meteorological conditions on pollution in the SCB.

Existing research on air pollution in the SCB has limited analyses of pollution characteristics to a specific year or causes of individual pollution events, and a summary of the long-term trends in winter $\text{PM}_{2.5}$ anthropogenic emission characteristics in the basin is lacking. Moreover, early studies on the impacts of meteorological conditions and anthropogenic emissions on $\text{PM}_{2.5}$ primarily focused on the changes in pollution levels from 2013 to 2020, particularly analyzing variations in certain key years. The quantification of anthropogenic emission impacts was based solely on observed values and meteorological influences, which precluded a quantitative assessment of the contributions of different regions and sectors to interannual $\text{PM}_{2.5}$ variations under the

combined effect of meteorology and emissions, making it difficult to determine the effectiveness of controlling anthropogenic emissions originating from specific regions and sources under certain extreme weather conditions. In this study, the WRF and CMAQ-ISAM models are employed to simulate the spatial distribution of the PM_{2.5} concentration during representative polluted winter months from 2002 to 2020, calculates the annual regional transport contributions and major anthropogenic source contributions among different cities within the SCB, and analyses their yearly patterns of variation. Finally, building on existing research on the impacts of meteorological conditions and anthropogenic emissions, in this study, the sources of winter PM_{2.5} in each simulated year are simulated and analyzed using the annual MEIC inventory. It aims to quantify the contributions of meteorological and emission factors to pollution sources in various regions and sectors. The findings elucidate the sources and contributions of transport to PM_{2.5} pollution in the SCB, providing a scientific basis for formulating more effective emission reduction policies.

2. Data and methods

2.1. WRF-CMAQ model configuration

The study's simulation period spanned from January of every third year from 2002 to 2020 (2002, 2005, 2008, 2011, 2014, 2017, and 2020) to represent the winter season. The annual meteorological fields from 2002 to 2020 were simulated using WRF v4.5.1 (Skamarock et al., 2019), with input data from the 0.25° × 0.25° Final Analysis (FNL) global reanalysis provided by the National Centers for Environmental Prediction (NCEP). The Moderate Resolution Imaging Spectroradiometer (MODIS) 2002–2020 MCD12Q1 land use data were used to update the subsurface static data so that the simulated results of the yearly meteorological field were closer to the actual conditions. The nested domains of the simulation, as shown in Fig. 1a, consisted of three levels, where the outermost domain (d01) covered most of China and its surrounding regions, with a spatial resolution of 54 km, and the innermost domain (d03) focused on the SCB, including parts of Eastern Sichuan Province and Chongqing (main urban area and northern areas in the basin), with a spatial resolution of 6 km. The related WRF parameterization schemes that were employed are detailed in Table 1.

Simulated annual winter PM_{2.5} concentrations were obtained using the CMAQ-ISAM v5.4 air quality model (USEPA, 2022), which matches the spatial domain of the WRF model. The chemical transport module

Table 1
WRF modeling configurations.

Model attribution	Configuration
Microphysics	Purdue Lin (Chen and Sun, 2002)
Longwave radiation	RRTM (Mlawer et al., 1997)
Shortwave radiation	RRTMG (Iacono et al., 2008)
Surface layer physics	Revised MM5 Monin-Obukhov
Land surface model	Noah Land Surface Model (Ek et al., 2003)
PBL physics scheme	MYJ (Noh et al., 2006)
Cumulus Parameterization	Kain-Fritsch (Kain, 2004)

employed the CB06 gas-phase chemistry mechanism (Luecken et al., 2019) and the AERO7 aerosol chemistry mechanism (Xu et al., 2018). Anthropogenic emissions inventory data were sourced from Tsinghua University's latest Multiresolution Emission Inventory for China (MEIC v1.4) (Li et al., 2017a; Zheng et al., 2018) and the 2010 MIX inventory (Li et al., 2017b), which included monthly average emissions data for seven years within the 2002–2020 period. The annual MEIC inventories were spatially allocated through coupling with the 2010 MIX inventory using the Inventory Spatial Allocation Tool (ISAT) model (Wang et al., 2023), yielding sector-specific (industrial, residential, agricultural, power, and transportation sources) anthropogenic emission inventories across nested domains for the model input (Wang et al., 2024). The inventory of the first layer was used to simulate the outer layer in conjunction with the boundary and initial conditions under CMAQ's default clean air condition, and the results of the pollutant concentrations that were obtained were then redistributed as input data for the boundary and initial conditions of the third layer to ensure that the external transport from the third layer was captured by the model (Feng et al., 2022; Qiao et al., 2019b).

Annual source apportionment and regional transport analyses were primarily conducted using CMAQ's Integrated Source Apportionment Method (ISAM), which tags emissions by source type and region, tracks them through the chemical transport module, and calculates the resulting concentrations and spatial distribution of target pollutants, as well as their contributions to overall pollutant levels. As an efficient refinement in source apportionment, ISAM results correlate with brute-force method outcomes with a coefficient >0.9 (Kwok et al., 2015). For PM_{2.5} emission source apportionment by region in the SCB, the region was divided into four main areas based on the method of Qiao et al. (2019a) (see Fig. 1b), including the two major cities in the western and eastern basin, namely, Chengdu (CD) and Chongqing (CQ), as well as the

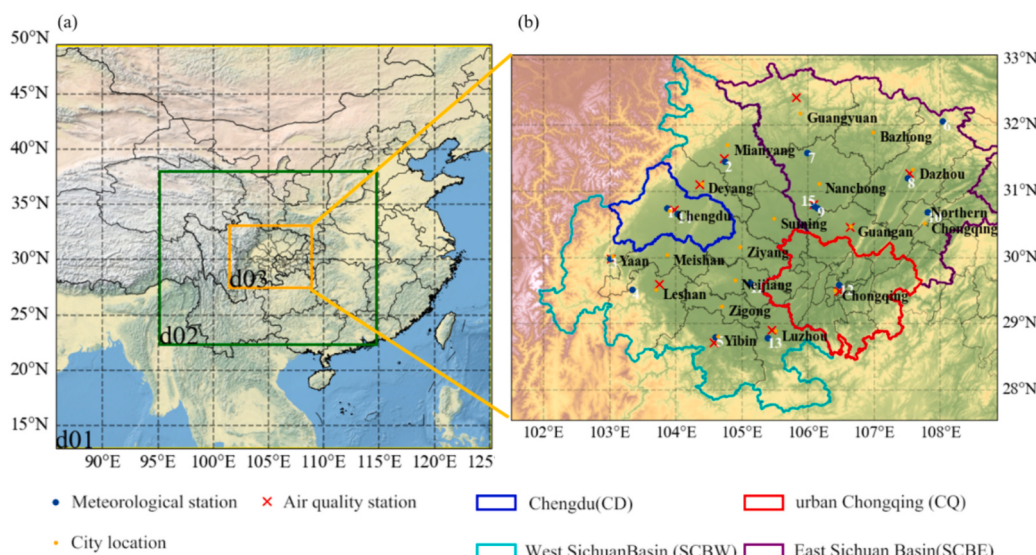


Fig. 1. The domains of the WRF-CMAQ simulation, showing the outermost layer (a) and the research area of the Sichuan Basin (b); the meteorological stations, environmental monitoring sites, prefecture-level city locations, and regional divisions are indicated in the figure.

western (SCBW, including Yaan, Meishan, Leshan, Deyang, Miyang, Suining, Ziyang, Neijiang, Zigong, Yibin, and Luzhou) and eastern (SCBE, including Guangyuan, Bazhong, Dazhou, Nanchong, Guangan, and northern Chongqing) prefecture-level cities, excluding Chengdu and Chongqing. Additionally, according to the default settings of the ISAM, $\text{PM}_{2.5}$ concentrations originating from boundary conditions and initial conditions were modeled separately, and the sum of their concentrations (BCIC) represented the additional human emissions outside the basin according to the method of boundary generation (Kitagawa et al., 2021; Zhang et al., 2023). For the source apportionment of $\text{PM}_{2.5}$ by emission sector, the tagged targets were the coupled anthropogenic sources in five sectors and encompassed the entire SCB.

The observational data for validation included hourly measurements of meteorological elements at stations within the SCB and ground-level $\text{PM}_{2.5}$ concentrations at environmental monitoring sites (Fig. 1b). Meteorological station data were sourced from the National Climatic Data Center (NCDC), and hourly $\text{PM}_{2.5}$ concentration data were obtained from the China Environmental Monitoring Center.

2.2. Calculation of contributions from meteorological conditions and anthropogenic emissions changes

This study utilized meteorological and anthropogenic emission data from January 2002–2020 and conducted sensitivity simulations with the CMAQ-ISAM model to quantify the yearly impacts of meteorological and emission changes on the winter $\text{PM}_{2.5}$ concentration, source apportionment, and regional transport (Shao et al., 2023; Wang et al., 2019; Wu et al., 2022). The specific calculation method was as follows: first, the actual $\text{PM}_{2.5}$ concentrations C_i for each year from 2002 to 2020 were simulated by modeling the meteorological fields and emission sources for the same year (Eq. 1). Afterward, the anthropogenic source emission inventories for 2011 were kept constant, and simulations were conducted using the meteorological fields for each year to obtain the simulated $\text{PM}_{2.5}$ concentration $C_i^{\text{Em}11}$ (Eq. 3) for each year under the emission conditions in 2011, which in turn allowed for the calculation of the amount of change in the simulated $\text{PM}_{2.5}$ concentration due to the change in meteorological conditions, $\Delta C_{ij}^{\text{Met}}$ (Eq. 5). The amount of change in modeled $\text{PM}_{2.5}$ concentrations due to changes in anthropogenic emissions was calculated from the difference in the amount of change in the concentrations (Eq. 4) in a given year compared to the 2011 emission conditions (Eq. 6).

$$C_i = \text{Met}_i \text{Em}_i \quad (1)$$

$$\Delta C_{ij} = \text{Met}_j \text{Em}_j - \text{Met}_i \text{Em}_i \quad (2)$$

$$C_i^{\text{Em}11} = \text{Met}_i \text{Em}_{11} \quad (3)$$

$$\Delta C_k^{\text{Em}11} = \text{Met}_k \text{Em}_k - \text{Met}_k \text{Em}_{11} \quad (4)$$

$$\Delta C_{ij}^{\text{Met}} = C_j^{\text{Em}11} - C_i^{\text{Em}11} = \text{Met}_j \text{Em}_{11} - \text{Met}_i \text{Em}_{11} \quad (5)$$

$$\Delta C_{ij}^{\text{Em}} = \Delta C_j^{\text{Em}11} - \Delta C_i^{\text{Em}11} = \Delta C_{ij} - \Delta C_{ij}^{\text{Met}} \quad (6)$$

Given that the core principle of ISAM involves assigning pollutant concentrations generated in the previous timestep to tagged pollutants in the current timestep based on certain weights, with the sum of the tagged $\text{PM}_{2.5}$ concentrations representing the total $\text{PM}_{2.5}$ concentration, it is possible to quantitatively compare the influence of meteorological conditions and changes in anthropogenic emissions on concentration levels for four regions and five sectors under both regional transport and source apportionment tagging scenarios (Eq. 7).

$$\Delta C_{ij} = \sum_x \Delta C_{ij}^{\text{region}_x} = \sum_x \Delta C_{ij}^{\text{emission}_x} \quad (7)$$

3. Results and discussion

3.1. Model performance evaluation

The evaluation of the accuracy of the simulated results of the model included both meteorological and environmental data. In the validation of the WRF model-simulated meteorological data, the selected parameters include the temperature (T2), wind speed (WS), wind direction (WD), and relative humidity (RH). This approach involved the use of daily mean simulated values for January in all simulation years, which were compared against available daily observed values at all 15 meteorological stations within the basin. Evaluation metrics, including the root mean square error (RSME), mean bias (MB), normalized mean bias (NMB), and normalized mean error (NME), were employed (Wang et al., 2014), and the results are listed in Table S1. Due to the availability of valid observed near-surface $\text{PM}_{2.5}$ concentrations in China starting in May 2014, the hourly winter $\text{PM}_{2.5}$ concentrations could be verified for the simulations of only 2017 and 2020, and based on related studies (Boylan and Russell, 2006; Emery et al., 2017; Huang et al., 2021), we selected the correlation coefficient (R), Normalized mean error (NME), Normalized mean bias (NMB), fractional error (FE), fractional bias (FB) and mean absolute error (MAE) as evaluation indices and referred to their benchmarks, and all parameters are calculated by combining the hourly series of observed and simulated values for 2017 and 2020.

Regarding the WRF validation results, the average RSME and MB for T2 across all sites were 2.09 and 0.88, respectively, with both the NMB and NME <20 %, indicating a satisfactory temperature simulation performance. For the wind speed, excluding the EMS station, the RMSE at all sites was <2 m/s, with an average MB of 0.69. The NMB and NME are comparable to those in Wang et al. (2014), suggesting that the overall bias in the wind speed simulations is generally reasonable. For the wind direction, due to its vector nature, the actual error between 0° and 360° was 0, but there was a numerical error (Zhang et al., 2006), leading to a large RSME of 90.86. The MB, NMB, and NME values were –1.26 %, 3.08 %, and 51.58 %, respectively. For the relative humidity (RH), the RSME was 24.64, and the MB fluctuated between 3.64 and –29.29 over the years. This underestimation of the RH has also been observed in related studies (Qiao et al., 2021; Yang et al., 2020). Moreover, the uncertainty in the meteorological field generally increases over a longer simulation period, resulting in a larger error in the RH. Overall, the simulation results for T2 and WS were favorable, while those for RH and WD are comparable to those of relevant studies. The model captured the winter meteorological field of the SCB in various years with reasonable accuracy.

To evaluate the performance of the CMAQ simulation, the selected parameters for hourly $\text{PM}_{2.5}$ concentrations in January of the winters of 2017 and 2020 were calculated (Table S2). The results indicated that the average FE and FB at the validation sites were 54.47 % and 4.98 %, respectively, meeting the criteria of Huang et al. (2021), namely, $\text{FB} < \pm 25\%$ and $\text{FE} < 55\%$. Regarding the parameter results at each site, all of them met the validation criteria of Boylan and Russell (2006), namely, $\text{FB} < \pm 60\%$ and $\text{FE} < 75\%$. The ranges of the MAE values for all the sites were 28.51–58.02, the average R value across all stations was 0.35, with NMB and NME averaging 54.89 % and 7.15 %, respectively. Due to the meteorological impacts associated with spatial location differences (Fig. 1b) and uncertainties in the emission inventory, the validation results for sites in the northeastern cities of the SCB were superior to those for sites in the southwestern cities. Additionally, the simulated concentration in the grid cells corresponds to the average concentration within the range of 6 km resolution, which is different from the spatial scale represented by the environmental monitoring stations, leading to a relatively low average R of 0.35 between the two. Overall, the model successfully simulated the distribution of $\text{PM}_{2.5}$ concentrations in the SCB during winter.

3.2. Changes in anthropogenic emission sources in the Sichuan Basin during winter from 2002 to 2020

Fig. 2 presents the total emissions for January across all simulated years within the SCB from the MEIC inventory, including PM_{2.5} and its major precursors, i.e., NO_x, SO₂, and NH₃, from five sectors (Liu et al., 2010). The January emission trends of the four pollutants were somewhat different, and from 2002 to 2020, the emissions of each sector of PM_{2.5} (**Fig. 2a**) showed a decreasing trend from year to year; among them, the highest emissions were from residential sources, followed by industrial sources, and the other three sectors accounted for a lower percentage of emissions. The emissions of NO_x (**Fig. 2b**) and SO₂ (**Fig. 2c**) both initially increased and then decreased, with SO₂ emissions substantially exceeding those of NO_x. The peak emissions occurred in 2008 for SO₂ and in 2011 for NO_x. Industrial, residential, and power sources all had significant shares of SO₂ and NO_x emissions, while transportation sources were a major contributor to NO_x emissions alone. According to national transportation department statistics, vehicle ownership in Chengdu has reached its second highest level in the country (Zhou et al., 2019), resulting in high NO_x emissions from traffic sources. NH₃ emissions have remained relatively stable, primarily originating from agricultural sources with secondary residential sources; this finding is consistent with the SCB being one of China's key agricultural regions. Analysis of the emission trends for the four pollutants indicated a general reduction in PM_{2.5} and its precursors in the SCB from January 2002 to 2020, with NO_x and SO₂ emissions showing an initial slow increase to a peak followed by a rapid decline.

3.3. Spatial variations in PM_{2.5} concentrations in the Sichuan Basin during winter from 2002 to 2020

Fig. 3 presents the spatial distribution of the monthly average PM_{2.5} concentrations obtained from the WRF–CMAQ simulations using actual meteorological fields and anthropogenic emission inventories for January of each year. Air stagnation due to basin topography restricted PM_{2.5} dispersion (Liao et al., 2018; Zhan et al., 2019), resulting in higher concentrations over seven simulated years, with peaks in the central SCB, east-central Chengdu, and western Chongqing. The western Sichuan Plateau had lower values, which is attributed to its high elevation and minimal human activities. For the spatial distribution in different years, in 2002, the high PM_{2.5} concentrations were mainly distributed in Chongqing and the central part of the SCB, and the urban area of Chongqing had the highest concentration (300 µg/m³) in all the

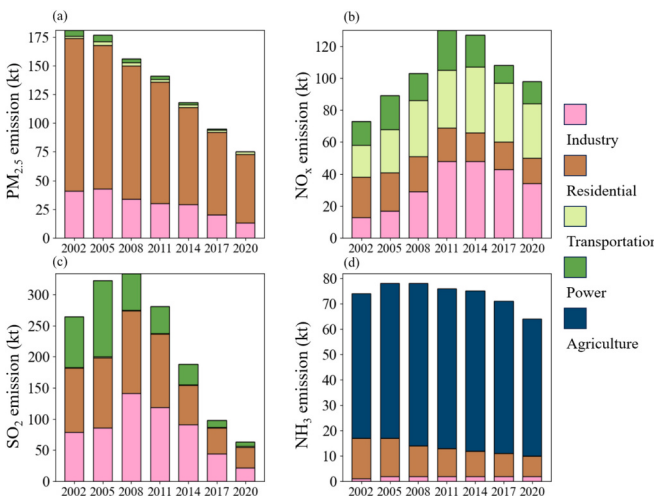


Fig. 2. In all the simulated years, the MEIC inventory included the total January emissions of PM_{2.5}, NO_x, SO₂, and NH₃ across five sectors within the Sichuan Basin.

years, while the western part of the Basin had a high concentration only in Chengdu. From 2002 to 2008, high PM_{2.5} concentrations in Chongqing were gradually concentrated in urban areas, while the PM_{2.5} concentrations in the western basin, excluding Chengdu, increased, with a generally slow decline in PM_{2.5} concentrations across the entire basin. Between 2011 and 2014, the PM_{2.5} concentrations in the SCB significantly increased compared to those in 2008, with high-value areas progressively concentrating around Chengdu, Chongqing, and the central region of the basin. During 2017 and 2020, the implementation of emission reduction policies from the Clean Air Action initiated in 2013, such as setting ultralow emission standards for coal-fired power plants, phasing out outdated industrial capacities, substituting residential coal use with electricity and natural gas, and strengthening vehicular emission standards (Zheng et al., 2018), resulted in a significant reduction in winter PM_{2.5} concentrations compared to all previous years. In 2017, the spatial distribution of the PM_{2.5} concentration was similar to that in 2014, but the high concentration decreased to 150 µg/m³. By 2020, the PM_{2.5} concentrations in the SCB further decreased compared to those in 2017, with the high-value pollution areas across the basin showing an approximately 50 % decrease from those in 2014.

Fig. 4 shows the triennial spatial distribution of the monthly mean changes in the PM_{2.5} concentration. The results indicate that from 2002 to 2020, in addition to a marked reduction in winter PM_{2.5} levels between 2014 and 2017 (**Fig. 4e**) and from 2017 to 2020 (**Fig. 4f**), there were varying degrees of increases or decreases in specific regions during other periods. Between 2002 and 2005, there was a notable decrease in the PM_{2.5} concentrations (up to 80 µg/m³) in the urban and northern areas of Chongqing, as opposed to significant increases (up to 100 µg/m³) in the western part of the SCB, particularly in Chengdu, Meishan, Leshan, and Yaan. From 2005 to 2008, changes in PM_{2.5} levels across the basin were relatively minor, with overall variations within ±20 µg/m³. Between 2008 and 2011, except for a decrease in PM_{2.5} concentrations in northern Chengdu and Deyang, other areas mainly experienced an increase. From 2011 to 2014, the PM_{2.5} concentrations in Chengdu and the central basin noticeably increased due to severe pollution events (Liao et al., 2017). In the period of significant PM_{2.5} reduction (2014 to 2020), the period from 2014 to 2017 experienced the greatest decrease in the western SCB, while from 2017 to 2020, the eastern part of the basin showed a clear reduction in PM_{2.5} concentrations, and the COVID-19 lockdown measures resulted in minimal spatial variation in the PM_{2.5} concentration across Chengdu, Chongqing, and the western basin, with no areas of relatively high pollution.

3.4. PM_{2.5} source apportionment and regional transport variability in the Sichuan Basin during winter from 2002 to 2020

3.4.1. Changes in regional contributions

Using the method of regional division shown in **Fig. 1**, the CMAQ-ISAM was further employed to simulate the absolute and relative contributions of the four designated areas to their own and other regions' monthly mean PM_{2.5} concentrations (**Fig. 5**), as well as to compile the spatial distribution (**Fig. S1**) and change in mean monthly PM_{2.5} concentrations across different regions (**Fig. S2**).

The results indicated that local emissions were the primary source of PM_{2.5} in the four regions, excluding boundary sources, with contribution rates initially decreasing and then increasing. For the SCBE, the primary regional sources of PM_{2.5} were predominantly local emissions from the Nanchong area and northern Chongqing and boundary sources, with minor impacts from other regions. The regional transport contribution from CD was significant mainly in 2002, but subsequently, the local and boundary sources became the dominant influences. All of the other three regions exhibited characteristics of interregional PM_{2.5} transport influences. CD was significantly affected by transport from SCBW; SCBW was more influenced by transport from SCBE; and CQ was mainly affected by transport from SCBW in 2002 but thereafter was primarily affected by transport from SCBE. In terms of the absolute contribution to

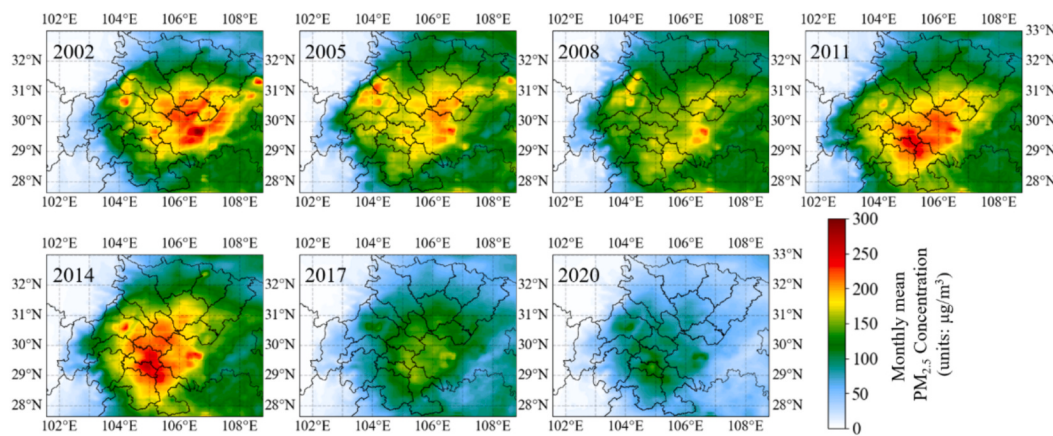


Fig. 3. Spatial distribution of the monthly mean $\text{PM}_{2.5}$ concentrations in January from 2002 to 2020 across the Sichuan Basin.

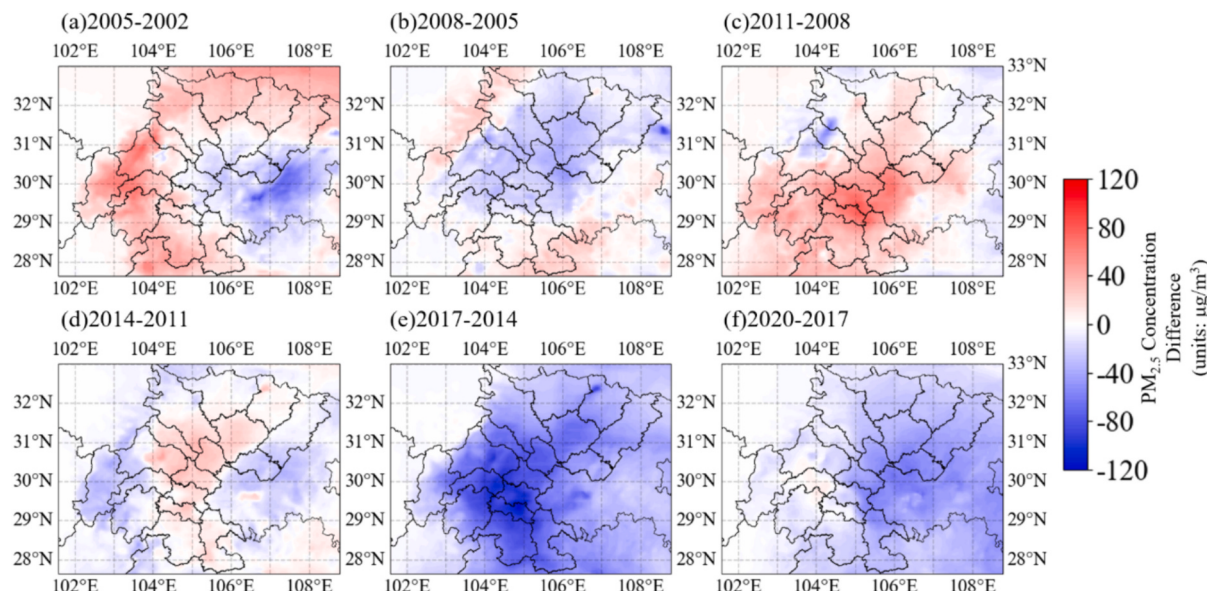


Fig. 4. Spatial distribution of changes in the mean January $\text{PM}_{2.5}$ concentration in the Sichuan Basin during winter from 2002 to 2020.

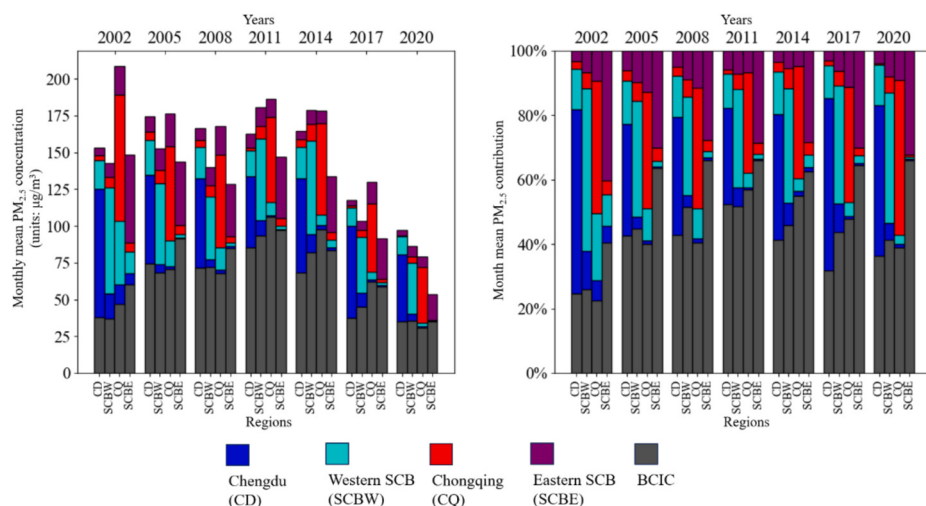


Fig. 5. Absolute and relative contributions of the monthly mean $\text{PM}_{2.5}$ concentrations among the designated regions and boundary conditions in the Sichuan Basin during winter from 2002 to 2020.

the PM_{2.5} concentration, the concentration in SCBE decreased from 148.39 µg/m³ in 2002 (similar to that in the CD and SCBW regions) to 53.51 µg/m³ in 2020, which was significantly lower than that in the other three regions. The disparity in the PM_{2.5} concentration between SCBW and CQ gradually decreased from 2002 to 2020. Prior to 2011, emissions in CQ decreased annually, while emissions in SCBW increased. After 2014, both regions began to experience a reduction in PM_{2.5} concentrations, with the emissions of CQ decreasing below those of SCBW by 2020. Compared to CD, CQ had the highest emissions within the basin in 2002 (208.56 µg/m³) and maintained slightly higher emissions than did CD from 2005 to 2017. However, by 2020, the emissions of CQ were lower than those of CD, which ultimately had the highest PM_{2.5} concentration among the four regions. Boundary sources consistently contributed the most to the SCBE. The absolute contributions of boundary sources to all four regions increased initially and then decreased, peaking during the rapid development of Eastern China from 2008 to 2011, prior to the implementation of China's air pollution control measures. From 2017 to 2020, a reduction in the absolute concentration contributions of the boundary sources was primarily observed in areas more susceptible to external transport, such as CQ and SCBE (approximately 25 µg/m³), while the changes in CD and SCBW were minimal. The spatial distribution of the reduction in boundary source contributions was more widespread across the four regions of the basin. This indicated that the nationwide COVID-19 lockdown in January 2020 significantly reduced national PM_{2.5} emissions, consequently decreasing the intensity of long-range transport pollution to the SCB.

3.4.2. Changes in the contributions of the five sectors

In the MEIC inventory, anthropogenic emission sources are categorized into five sectors: industrial, residential, agricultural, power, and transport. In this study, the monthly average spatial distribution for each of the five emission sources in the SCB was obtained for the simulated years (Fig. S3), their variations (Fig. S4), and their absolute and relative contributions to PM_{2.5} concentrations in the four designated regions (Fig. 6) using the ISAM tagging approach.

The results showed that residential sources were the main sources of PM_{2.5} emissions in all regions of the SCB from 2002 to 2020 (with relative contributions ranging from 21.50 % to 48.60 %), followed by industrial sources (5.10 % to 32.86 %), with agricultural, electric power, and transportation sources accounting for a relatively low share. The temporal variations in emission sources in the four regions were generally consistent with the trend of the total emissions, which all

exhibited a downward trend. The high-value distribution areas for residential and agricultural sources were relatively widespread; however, the quantity of emissions from residential sources was significantly greater than that from agricultural sources. The high-value impact areas of power and industrial sources were more localized and were primarily concentrated in the southern part of the SCB and the Chongqing region. For transportation emissions, except for Chongqing in 2002, high-value areas in other years were predominantly located in Chengdu and the western part of the SCB.

Comparing the relative and absolute contributions of different emission sources across regions, with the urbanization-driven transition from solid to clean fuels (Shen et al., 2017), the rates of contribution from residential sources in all four regions continuously decreased over the studied years. The highest average relative contribution rate decreased from 46.46 % in 2002 to 27.36 %, with the absolute contribution amount also decreasing by an average of approximately 65 µg/m³. The relative contribution rate of the second emission source, i.e., industrial, remained relatively stable over several years in the SCBE and SCBW regions, with the absolute concentration from that contribution source decreasing in the SCBE area. For CD and CQ, the relative contribution rate of industrial sources increased in both areas, with CD exceeding CQ in 2014 and 2017, and by 2020, the rates in both areas had once again become similar. The industrial emissions in the CD area were relatively high in 2014 and 2017 but did not exhibit a marked decrease in 2020 compared to those in 2002. Conversely, CQ had the lowest annual industrial emissions in 2020. An analysis of the two primary PM_{2.5} emission sources indicates that in the urban areas of CD and CQ, industrial and residential emissions contributed equally during the most recent period. In contrast, in SCBW and SCBE, residential emissions continued to dominate. Emissions from power sources have consistently remained low, becoming negligible for the PM_{2.5} emissions in all four regions since 2017. Moreover, contributions from transportation and agricultural sources have remained low and stable over the years.

3.5. Impacts of meteorological conditions and anthropogenic emissions on PM_{2.5} concentrations in the Sichuan Basin during winter from 2000 to 2020

Investigating the impact of meteorological conditions and anthropogenic emissions on PM_{2.5} concentrations over the years is crucial for understanding the distribution patterns in the SCB, and it provides guidance for the formulation of future environmental management policies. Fig. 7 presents the statistical results of the January mean PM_{2.5}

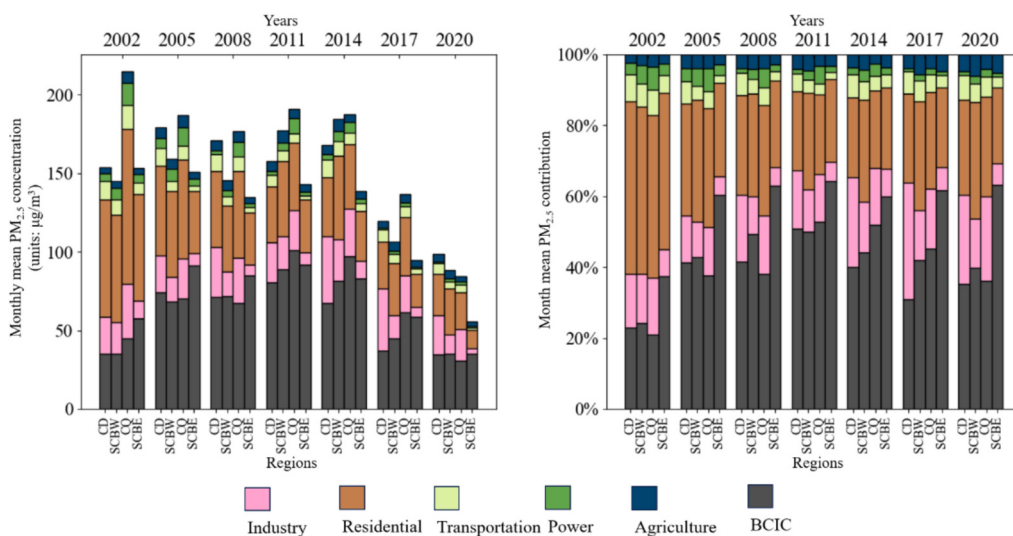


Fig. 6. Absolute and relative contributions of the monthly mean PM_{2.5} concentrations among the 5 sectors and boundary conditions in the Sichuan Basin during winter from 2002 to 2020.

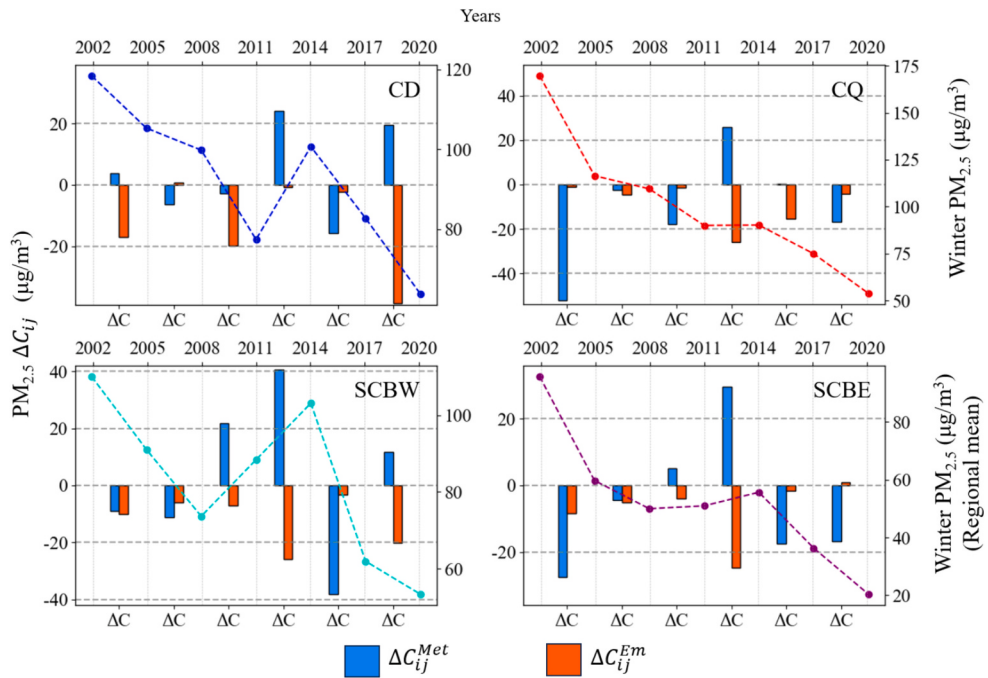


Fig. 7. Statistical results of the changes in January mean PM_{2.5} concentrations across four regions in the Sichuan Basin from 2002 to 2020 due to meteorological conditions and anthropogenic emissions.

concentration changes in four regions due to overall meteorological conditions and changes in anthropogenic emissions in area d03, while Fig. 8 illustrates the corresponding spatial distribution. The county-level variations are shown in Fig. S5. The monthly mean distributions of key meteorological factors (boundary layer height, temperature, relative humidity, and wind speed) are depicted in Fig. S6, and their change statistics are presented in Fig. S7. We further calculated the influence of changes in meteorological conditions and anthropogenic emissions from five sectors on PM_{2.5} concentrations across four regions to assess the sensitivity of different areas and pollution sources to these two factors. The results are displayed in Figs. 9 and 10. Since the initial and boundary conditions (BCIC) represent long-range transport from outside the SCB and are unrelated to the local meteorological fields within the basin, the impact of the BCIC on concentrations was not considered in any of the results.

3.5.1. Overall impacts on the four regions

Within the main regions of the SCB, changes in anthropogenic emissions generally made a negative contribution to the PM_{2.5} concentration, except in certain municipalities where positive contributions were observed from 2014 to 2020. Significant reductions were noted from 2011 to 2014 and from 2017 to 2020. The first period of decline coincided with the implementation of China's air pollution control policies in 2013, while the second period correlated with the implementation of COVID-19 pandemic control measures in 2020 (Zheng et al., 2021). The spatial distribution of changes in anthropogenic emissions primarily manifests in two scenarios: a reduction in PM_{2.5} concentrations at specific county and city points and a decrease in overall PM_{2.5} levels across the basin. The former is evident in the human emission reductions in the southern part of the SCB and the Deyang-Mianyang area of the SCBW from 2002 to 2011 and in the Nanchong and Chongqing areas from 2014 to 2017. The latter is reflected during the emission reduction implementation periods of 2011 to 2014 and 2017 to 2020, with the most notable decrease in PM_{2.5} concentrations across the SCBW region.

Relevant studies have shown that the meteorological field in winter has a stronger effect on PM_{2.5} accumulation and removal as well as

transport and stagnation compared to changes in emission sources, while the spatial extent of the effect of meteorological conditions on PM_{2.5} concentrations is wider (Tai et al., 2010; Wang et al., 2018b), which makes it possible that even with sustained emission reductions of pollutants, heavy pollution events can still occur as a result of unfavorable meteorological conditions. Calculations of the quantitative effects of meteorological conditions on PM_{2.5} concentrations in this study show that for the basin overall, meteorological conditions increased PM_{2.5} concentrations from 2008 to 2014. According to the meteorological field distribution characteristics for 2011 and 2014 (Fig. S5), the RH values were notably lower in these years than in other years, with areas with low RH values coinciding with increased pollution and a significant reduction in wind speed. According to related studies, RH and PM_{2.5} concentrations in southern China and the SCB showed a negative correlation, i.e., low relative humidity weakened the removal and diffusive effect of precipitation and onshore winds on PM_{2.5} (Leung et al., 2018), which caused unfavorable meteorological conditions to aggravate the degree of PM_{2.5} pollution, e.g., the increase in the PM_{2.5} concentration in the SCBW could reach 40 μg/m³, and the increase in the PM_{2.5} concentration in the SCBE could exceed 20 μg/m³. The increase in the PM_{2.5} concentration in the remaining three areas was also >20 μg/m³. In contrast, in 2017, there was an overall increase in RH compared to that in 2014, resulting in negative PM_{2.5} concentration changes across the basin due to meteorological factors, with the SCBW decreasing nearly 40 μg/m³, highlighting it as the region most affected by meteorological conditions. Regarding the degree of impact, the PM_{2.5} concentration changes from 2002 to 2005 and 2011–2017 were significantly greater than those in the other periods. Consistent with the negative correlation between the boundary layer height and pollution levels (Liu et al., 2021b), the SCBE and CQ regions exhibited a notable increase in the boundary layer height in 2005, a significant decrease in the basin-wide planetary boundary layer height (PBLH) in 2014 compared to that in 2011, and an increase again in 2017. These fluctuations align with changes in PM_{2.5} concentrations, indicating that boundary layer conditions are key factors affecting PM_{2.5} pollution in the SCB.

Geographical features result in varied meteorological and emission

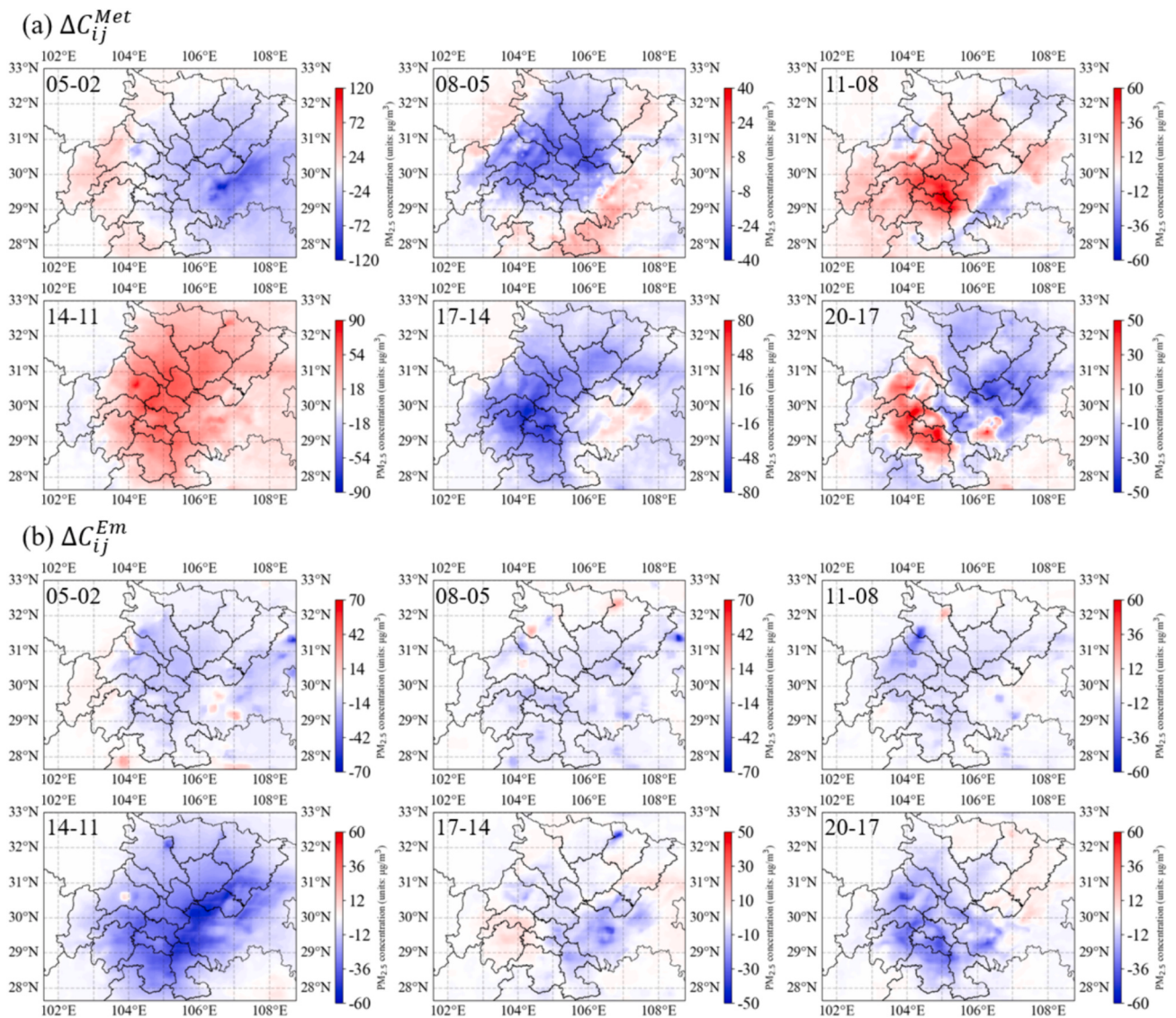


Fig. 8. Spatial distribution of changes in the January mean PM_{2.5} concentration in the Sichuan Basin from 2002 to 2020 due to meteorological conditions (a) and anthropogenic emissions (b).

influences across regions. As indicated by Fig. S5, the SCBW area, which is located on the expansive plains of the SCB and has a relatively lower urban density than the CD area, demonstrated a notably stronger meteorological impact on the PM_{2.5} concentration than did the other basin areas from 2008 to 2017. The variation in the boundary layer height in the CQ region was negatively correlated with its meteorological impact, with frequent calm wind pollution events due to the mismatch between upper-level and surface wind speeds caused by mountainous terrain, making the boundary layer a dominant factor in pollution (Guo et al., 2022). Between 2017 and 2020, the SCBW and CD, located in the downwind and plain areas, experienced air masses transported from the eastern CQ and SCBE along the basin's edge to the southwest, accumulating on the slopes of the Yunnan–Guizhou Plateau. The terrain-induced vertical movements between Longquan Mountain and Huaying Mountain led to opposite meteorological impacts on PM_{2.5} concentrations between the eastern and western parts (Liu et al., 2021a).

Comparing the overall concentration changes to those influenced by anthropogenic emissions, the implementation of COVID-19 lockdown measures in urban areas of the SCB from 2017 to 2020 resulted in a quantitative spatial reduction in PM_{2.5} similar to that between 2011 and 2014. The primary affected regions were SCBW, CD, and CQ, which are

three closely interconnected urban clusters. However, due to the adverse meteorological conditions causing internal pollution transport within the basin, the overall PM_{2.5} concentration did not significantly decrease as a result of the lockdown. In contrast, the SCBE region exhibited a reduction in PM_{2.5} pollution not due to a decrease in anthropogenic emissions but rather due to long-range transport, suggesting that short-term forced emission reductions may not yield significant results due to meteorological influences.

3.5.2. Impacts of the four regions on each other

Fig. 9 reveals that changes in PM_{2.5} concentrations across the four regions due to varying meteorological conditions are mixed, showing no clear trend. In contrast, changes due to anthropogenic emissions are predominantly negative, underscoring the greater influence of meteorological conditions on PM_{2.5} levels than that of human emissions.

Fig. 9(a) shows that PM_{2.5} concentration changes due to meteorological conditions in basins vary regionally. The alterations in the meteorological conditions in SCBW had a relatively greater impact on its own PM_{2.5} levels and those of the three other regions, followed by those of the SCBE and CD areas. CQ significantly influenced its own PM_{2.5} levels during 2002–2005, with weaker impacts in other periods.

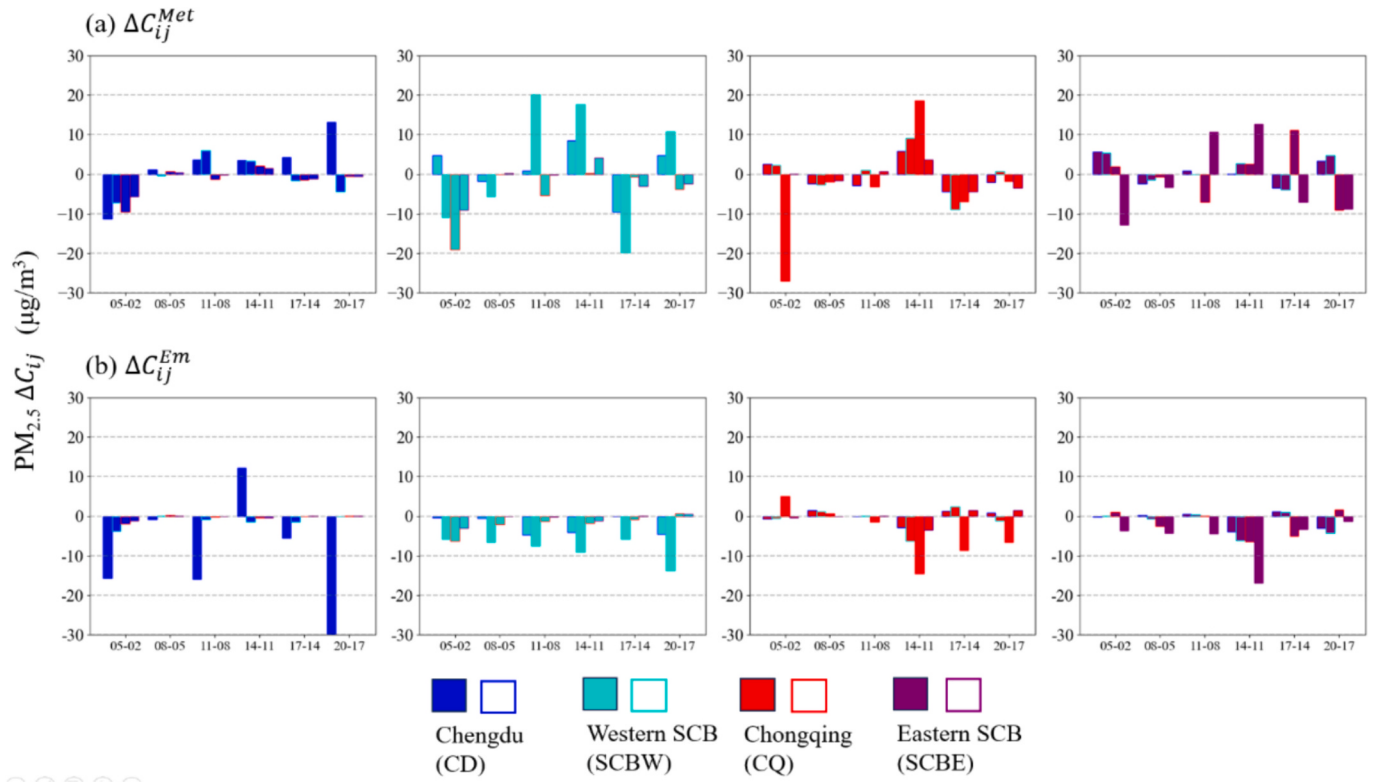


Fig. 9. Statistical results of changes in January mean PM_{2.5} concentrations for four regions from 2002 to 2020 due to changes in meteorological conditions (a) and total anthropogenic emissions (b). The solid bars indicate the regions with changes in meteorological conditions and anthropogenic emissions, and the hollow bars show the impacted regions.

Combined with the annual wind field distribution (Fig. S6), the SCBE, located in the upwind area, has been identified as a major regional pollution source for the SCB (Liu et al., 2021a). The SCBW region exhibits high interannual variability similar to that of the SCBE region. A comprehensive analysis of the regional transport impacts in Fig. 9(a) provides an explanation for the overall results shown in Fig. 7: (1) from 2002 to 2005, the significant decrease in the PM_{2.5} concentration in CQ was due to reduced regional pollution transport from CD and SCBW under the influence of favorable meteorological conditions, coupled with beneficial local meteorological conditions in CQ; (2) from 2011 to 2014, the increase in PM_{2.5} levels in CD and SCBW was due to unfavorable meteorological conditions in SCBE and CQ.

Fig. 9(b) indicates that reductions in anthropogenic emissions in the CD region primarily affect its own PM_{2.5} concentrations, while decreases in emissions from the other three regions result in more pronounced interregional influences on PM_{2.5} levels. The reduction in anthropogenic emissions from SCBE predominantly affects itself and CQ. The decrease in emissions from SCBW primarily influenced CQ and SCBE before 2005 and CD after 2011, suggesting a closer developmental link between CD and the western basin city cluster after 2011. Overall, the reduction in PM_{2.5} concentrations in most cities within the basin from 2011 to 2014 following the implementation of air pollution control policies mainly resulted from the combined impact of SCBW, CQ, and SCBE, with minimal influence from CD.

3.5.3. Impact of five sectors across four regions

Fig. 10 shows that the changes in the PM_{2.5} concentrations associated with industrial and residential sources ($\pm 30 \mu\text{g}/\text{m}^3$) exceeded those associated with the other three emission sources ($\pm 5 \mu\text{g}/\text{m}^3$). Considering the impact of meteorological conditions on the PM_{2.5} concentrations in the five sectors (Fig. 10(a)), the data combined with Fig. S7 indicate that from 2011 to 2014, adverse meteorological conditions due to a low boundary layer height significantly increased the PM_{2.5}

concentration from all but agricultural sources, particularly in the SCBW region. The predominant distribution of agricultural sources in rural areas and that of other sources mainly in urban areas suggests a marked difference in boundary layer height conditions between urban and rural zones of the SCB. In other years, changes in PM_{2.5} concentrations from the five sectors were influenced by a combination of meteorological conditions, generally leading to a decrease in PM_{2.5} levels. PM_{2.5} concentration changes due to emissions from five sectors show that industrial sources have a more significant impact on CD and CQ than on the other regions, with an increase in PM_{2.5} concentrations before 2014 followed by a subsequent decrease. Changes in PM_{2.5} concentrations due to residential sources, on the other hand, show a continuous basin-wide decrease; changes in PM_{2.5} concentrations due to the remaining three sources have smaller values, and changes in PM_{2.5} concentrations are dominated by decreases, except for agricultural sources.

Compared to Fig. 9, it is evident that in certain years, changes in PM_{2.5} concentrations in the CQ region due to emissions from the five sectors within the basin were significantly greater than those caused by local emissions in CQ, further indicating the role of regional transport in contributing to PM_{2.5} pollution in the CQ area. The primary contribution of industry to PM_{2.5} pollution is through the secondary transformation of emitted SO₂ (Wang et al., 2018a), and with SO₂ emissions consistently rising from 2002 to 2008 according to the MEIC inventory (Fig. 2), industrial sources in the CQ region made a positive contribution to anthropogenic emissions during this period. From 2002 to 2011, urbanization in the CD region progressed more slowly than that in the CQ region, resulting in fewer impacts from industrial and transportation sources. However, higher PM_{2.5} concentration changes due to residential sources suggest that the decline in PM_{2.5} concentrations during this period was primarily driven by reductions in emissions from residential sources. After 2011, despite the acceleration of urbanization in CD, emissions from industrial and transportation sources did not lead to an increase in PM_{2.5} concentrations due to the implementation of effective

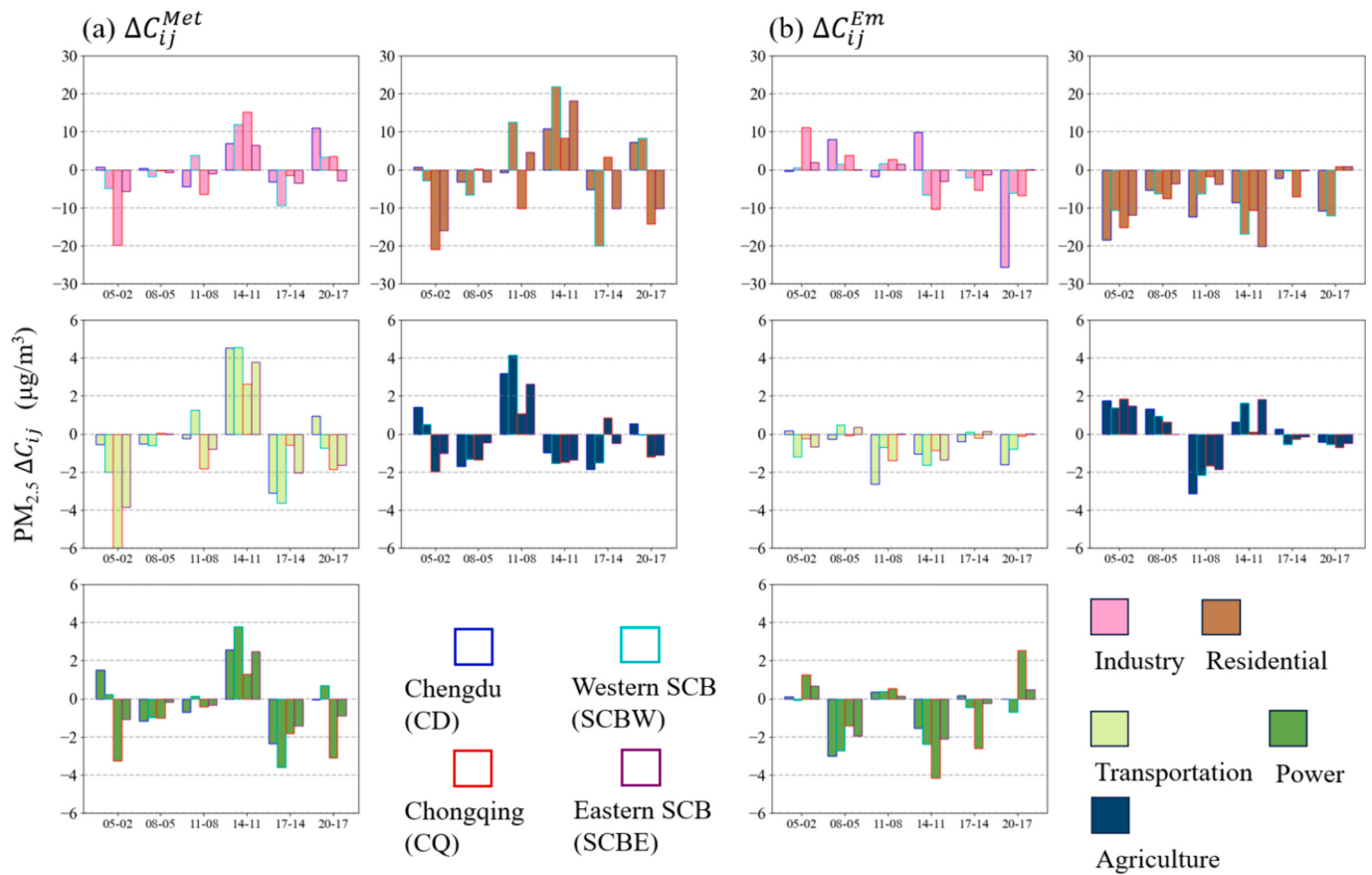


Fig. 10. Statistical results of changes in January mean $\text{PM}_{2.5}$ concentrations for five sectors across four regions from 2002 to 2020 due to changes in meteorological conditions (a) and total anthropogenic emissions (b). The solid bars indicate the sectors with changes in meteorological conditions and anthropogenic emissions, and the hollow bars show the impacted regions.

air pollution control policies. For the SCBW and SCBE regions, the $\text{PM}_{2.5}$ concentration changes due to industrial emissions were minimal under both conditions, indicating that less-developed urban areas have weaker industrial emission controls than more-developed urban regions.

4. Conclusions

This study employed the WRF–CMAQ model, together with the ISAM, to simulate and analyze winter $\text{PM}_{2.5}$ concentration trends in the SCB from 2002 to 2020 influenced by meteorological conditions and human emissions. The main conclusions are as follows:

- (1) From 2002 to 2020, the winter $\text{PM}_{2.5}$ concentrations in the SCB showed a decreasing trend, from a peak of $300 \mu\text{g}/\text{m}^3$ to $120 \mu\text{g}/\text{m}^3$. Significant changes in the annual concentration occurred from 2002 to 2008 and 2014–2020; the former could be attributed to the decreasing influence of unfavorable meteorological conditions in the Chongqing region, while the latter reflected the effectiveness of pollution control policies in China. Spatially, the primary pollution areas shifted from an initial center on Chongqing to Chengdu and the western part of the basin, with an eventual decrease across the entire basin.
- (2) In terms of regional transport, local emissions and boundary sources significantly contributed to all four areas. SCBE was influenced primarily by CQ and boundary sources, whereas the other three regions were more heavily affected by each other, with the influence changing over time. In terms of absolute contribution, CQ was the highest in 2002 ($208.56 \mu\text{g}/\text{m}^3$), and SCBE was the lowest in 2020 ($53.51 \mu\text{g}/\text{m}^3$). In the source

apportionment of the five sectors, residential emissions were the main source of $\text{PM}_{2.5}$ in the basin (ranging from 21.50 % to 48.60 %), followed by industrial emissions (ranging from 5.10 % to 32.86 %). Residential source contributions decreased annually due to energy structure transitions, with SCBW and SCBE being the primary emission areas, while industrial emissions were mainly centered on CD and CQ.

- (3) Meteorological conditions can exacerbate or alleviate $\text{PM}_{2.5}$ pollution in the basin, contingent upon basin-wide adverse meteorological conditions, the boundary layer height in the hilly regions of CQ, and the influence of upwind winds on the Chengdu Plain area. The contribution of anthropogenic emissions to $\text{PM}_{2.5}$ decreased annually, mainly due to the implementation of relevant atmospheric pollution control policies. The cities of CD and CQ were less affected by meteorological factors, with local emission controls showing significant reduction effects. For SCBE and SCBW, meteorological conditions jointly impacted other areas, with the SCBE being closely related to CQ, and the influence of SCBW on the western part of the basin gradually surpassed that on the eastern part over time. Meteorological conditions had a greater influence on $\text{PM}_{2.5}$ concentrations from industrial and residential sources than did the other three types of sources ($\pm 30 \mu\text{g}/\text{m}^3$ vs. $\pm 5 \mu\text{g}/\text{m}^3$).

Building upon the aforementioned discussion, within the context of rapid urban expansion from 2002 to 2020 (Wang et al., 2022), Chengdu has overtaken Chongqing as the primary city influencing pollution in the SCB, with increased contributions of local emissions becoming a major characteristic of expanding cities. $\text{PM}_{2.5}$ transport in the SCB region in

winter gradually decreased between east and west, indicating that the key to controlling PM_{2.5} pollution across the SCB region lies in implementing emission reductions in Chengdu to mitigate stagnation-type pollution in the western basin area and monitoring national pollution patterns to prevent contamination in the eastern basin area. Despite ongoing emission reduction efforts, severe pollution events may still occur due to adverse meteorological conditions. Urban pollution analyses within basins should not only focus on environmental characteristics but also on sensitive local meteorological factors.

CRediT authorship contribution statement

Yaohan Xian: Writing – original draft, Visualization, Project administration, Methodology, Investigation, Formal analysis, Conceptualization. **Yang Zhang:** Writing – review & editing, Project administration, Conceptualization. **Zhihong Liu:** Project administration, Conceptualization. **Haofan Wang:** Resources, Data curation, Conceptualization. **Tianxin Xiong:** Data curation.

Declaration of competing interest

The authors declare no conflict of interest.

Data availability

Data will be made available on request.

Acknowledgments

This study was supported by the National Key Research and Development Program of China (No. 2023YFC3709301), the Sichuan Science and Technology Program (2023YFS0383 and 2023NSFSC0745), the Chengdu Science and Technology Project (2022-YF05-00770-SN), the Unveiling and Commanding Technology Project of Longquanyi District, Chengdu (2023LQYF0011), the National Natural Science Foundation of China (41901294), and the College Students' Innovative Entrepreneurial Training Plan Program (202310621360).

Appendix A. Supplementary data

Supplementary data to this article can be found online at <https://doi.org/10.1016/j.scitotenv.2024.174557>.

References

- An, Z., Huang, R.J., Zhang, R., Tie, X., Li, G., Cao, J., Ji, Y., 2019. Severe haze in northern China: a synergy of anthropogenic emissions and atmospheric processes. *Proc. Natl. Acad. Sci. USA* 116 (18), 8657–8666. <https://doi.org/10.1073/pnas.1900125116>.
- Bellouin, N., Quaas, J., Gryspenert, E., Kinne, S., Stier, P., Watson-Parris, D., Daniell, A.L. J.R., o. G., 2020. Bounding Global Aerosol Radiative Forcing of Climate Change 58 (1), e2019RG000660.
- Boylan, J.W., Russell, A.G., 2006. PM and light extinction model performance metrics, goals, and criteria for three-dimensional air quality models. *Atmos. Environ.* 40 (26), 4946–4959. <https://doi.org/10.1016/j.atmosev.2005.09.087>.
- Chang, X., Wang, S., Zhao, B., Xing, J., Liu, X., Wei, L., Zheng, M., 2019. Contributions of inter-city and regional transport to PM(2.5) concentrations in the Beijing-Tianjin-Hebei region and its implications on regional joint air pollution control. *Sci. Total Environ.* 660, 1191–1200. <https://doi.org/10.1016/j.scitotenv.2018.12.474>.
- Chen, S.-H., Wan, W.-Y., 2002. A One-dimensional Time Dependent Cloud Model. *Journal of the Meteorological Society of Japan. Ser. II* 80 (1), 99–118. <https://doi.org/10.2151/jmsj.80.99>.
- Cheng, J., Su, J., Cui, T., Li, X., Dong, X., Sun, F., He, K., 2019. Dominant role of emission reduction in PM_{2.5} air quality improvement in Beijing during 2013–2017: a model-based decomposition analysis. *Atmos. Chem. Phys.* 19 (9), 6125–6146. <https://doi.org/10.5194/acp-19-6125-2019>.
- Deng, C., Tian, S., Li, Z., Li, K., 2022. Spatiotemporal characteristics of PM(2.5) and ozone concentrations in Chinese urban clusters. *Chemosphere* 295, 133813. <https://doi.org/10.1016/j.chemosphere.2022.133813>.
- Ek, M.B., Mitchell, K.E., Lin, Y., Rogers, E., Grunmann, P., Koren, V., Tarpley, J.D., 2003. Implementation of Noah land surface model advances in the National Centers for environmental prediction operational mesoscale eta model. *J. Geophys. Res. Atmos.* 108 (D22) <https://doi.org/10.1029/2002jd003296>.
- Emery, C., Liu, Z., Russell, A.G., Odman, M.T., Yarwood, G., Kumar, N., 2017. Recommendations on statistics and benchmarks to assess photochemical model performance. *J. Air Waste Manage. Assoc.* 67 (5), 582–598. <https://doi.org/10.1080/10962247.2016.1265027>.
- Feng, S., Jiang, F., Wang, H., Shen, Y., Zheng, Y., Zhang, L., Ju, W., 2022. Anthropogenic emissions estimated using surface observations and their impacts on PM(2.5) source apportionment over the Yangtze River Delta, China. *Sci. Total Environ.* 828, 154522. <https://doi.org/10.1016/j.scitotenv.2022.154522>.
- Gao, C., Zhang, X., Wang, W., Xiu, A., Tong, D., Chen, W., 2018. Spatiotemporal distribution of satellite-retrieved ground-level PM2.5 and near real-time daily retrieval algorithm development in Sichuan Basin, China. *Atmosphere* 9 (2). <https://doi.org/10.3390/atmos9020078>.
- Geng, G., Zheng, Y., Zhang, Q., Xue, T., Zhao, H., Tong, D., Hong, C.J.N.G., 2021. Drivers of PM_{2.5} air pollution deaths in China 2002–2017, 14 (9), 645–650.
- Gonzalez-Salazar, M.A., Kirsten, T., Prchlik, L., 2018. Review of the operational flexibility and emissions of gas- and coal-fired power plants in a future with growing renewables. *Renew. Sust. Energ. Rev.* 82, 1497–1513. <https://doi.org/10.1016/j.rser.2017.05.278>.
- Guo, Q., Wu, D., Yu, C., Wang, T., Ji, M., Wang, X., 2022. Impacts of meteorological parameters on the occurrence of air pollution episodes in the Sichuan basin. *J. Environ. Sci. (China)* 114, 308–321. <https://doi.org/10.1016/j.jes.2021.09.006>.
- He, K., Yang, F., Ma, Y., Zhang, Q., Yao, X., Chan, C.K., Mulawa, P., 2001. The characteristics of PM2.5 in Beijing, China. *Atmos. Environ.* 35 (29), 4959–4970. [https://doi.org/10.1016/s1352-2310\(01\)00301-6](https://doi.org/10.1016/s1352-2310(01)00301-6).
- He, Q., Zhang, M., Huang, B.J.A.E., 2016. Spatio-temporal variation and impact factors analysis of satellite-based aerosol optical depth over China from 2002 to 2015, 129, pp. 79–90.
- Huang, L., Zhu, Y., Zhai, H., Xue, S., Zhu, T., Shao, Y., Li, L., 2021. Recommendations on benchmarks for numerical air quality model applications in China – Part 1: PM_{2.5} and chemical species. *Atmos. Chem. Phys.* 21 (4), 2725–2743. <https://doi.org/10.5194/acp-21-2725-2021>.
- Huang, Q., Cai, X., Song, Y., Zhu, T., 2017. Air stagnation in China (1985–2014): climatological mean features and trends. *Atmos. Chem. Phys.* 17 (12), 7793–7805. <https://doi.org/10.5194/acp-17-7793-2017>.
- Iacono, M.J., Delamere, J.S., Mlawer, E.J., Shephard, M.W., Clough, S.A., Collins, W.D., 2008. Radiative forcing by long-lived greenhouse gases: calculations with the AER radiative transfer models. *J. Geophys. Res. Atmos.* 113 (D13) <https://doi.org/10.1029/2008jd009944>.
- Kain, J.S., 2004. The Kain–Fritsch Convective Parameterization: An Update. *J. Appl. Meteorol.* 43 (1), 170–181. [https://doi.org/10.1175/1520-0450\(2004\)043<0170:TKfp>2.0.Cz2](https://doi.org/10.1175/1520-0450(2004)043<0170:TKfp>2.0.Cz2).
- Kitagawa, Y.K.L., Pedruzzini, R., Galvão, E.S., de Araújo, I.B., Albuquerque, T. T.d.A., Kumar, P., Moreira, D.M., 2021. Source apportionment modelling of PM2.5 using CMAQ-ISAM over a tropical coastal-urban area. *Atmospheric Pollut. Res.* 12 (12) <https://doi.org/10.1016/j.apr.2021.101250>.
- Kwok, R.H.F., Baker, K.R., Napelenok, S.L., Tonneisen, G.S., 2015. Photochemical grid model implementation and application of VOC, NO_x, and O₃ source apportionment. *Geosci. Model Dev.* 8 (1), 99–114. <https://doi.org/10.5194/gmd-8-99-2015>.
- Lang, J., Cheng, S., Li, J., Chen, D., Zhou, Y., Wei, X., Wang, H., 2013. A monitoring and modeling study to investigate regional transport and characteristics of PM2.5 pollution. *Aerosol Air Qual. Res.* 13 (3), 943–956. <https://doi.org/10.4209/aaqr.2012.09.0242>.
- Leung, D.M., Tai, A.P.K., Mickley, L.J., Moch, J.M., van Donkelaar, A., Shen, L., Martin, R.V., 2018. Synoptic meteorological modes of variability for fine particulate matter (PM2.5) air quality in major metropolitan regions of China. *Atmos. Chem. Phys.* 18 (9), 6733–6748. <https://doi.org/10.5194/acp-18-6733-2018>.
- Li, M., Liu, H., Geng, G., Hong, C., Liu, F., Song, Y., He, K., 2017a. Anthropogenic emission inventories in China: a review. *Natl. Sci. Rev.* 4 (6), 834–866. <https://doi.org/10.1093/nsr/nwx150>.
- Li, M., Zhang, Q., Kurokawa, J.-I., Woo, J.-H., He, K., Lu, Z., Zheng, B., 2017b. MIX: a mosaic Asian anthropogenic emission inventory under the international collaboration framework of the MICS-Asia and HTAP. *Atmos. Chem. Phys.* 17 (2), 935–963. <https://doi.org/10.5194/acp-17-935-2017>.
- Li, R., Mei, X., Wei, L., Han, X., Zhang, M., Jing, Y., 2019. Study on the contribution of transport to PM2.5 in typical regions of China using the regional air quality model RAMS-CMAQ. *Atmos. Environ.* 214 <https://doi.org/10.1016/j.atmosenv.2019.116856>.
- Li, X., Hussain, S.A., Sobri, S., Md Said, M.S., 2021. Overviewing the air quality models on air pollution in Sichuan Basin, China. *Chemosphere* 271, 129502. <https://doi.org/10.1016/j.chemosphere.2020.129502>.
- Liao, T., Wang, S., Ai, J., Gui, K., Duan, B., Zhao, Q., Sun, Y., 2017. Heavy pollution episodes, transport pathways and potential sources of PM(2.5) during the winter of 2013 in Chengdu (China). *Sci. Total Environ.* 584–585, 1056–1065. <https://doi.org/10.1016/j.scitotenv.2017.01.160>.
- Liao, T., Gui, K., Jiang, W., Wang, S., Wang, B., Zeng, Z., Sun, Y., 2018. Air stagnation and its impact on air quality during winter in Sichuan and Chongqing, southwestern China. *Sci. Total Environ.* 635, 576–585. <https://doi.org/10.1016/j.scitotenv.2018.04.122>.
- Liu, J., Zheng, Y., Geng, G., Hong, C., Li, M., Li, X., Zhang, Q., 2020. Decadal changes in anthropogenic source contribution of PM_{2.5} pollution and related health impacts in China, 1990–2015. *Atmos. Chem. Phys.* 20 (13), 7783–7799. <https://doi.org/10.5194/acp-20-7783-2020>.
- Liu, X.-H., Zhang, Y., Xing, J., Zhang, Q., Wang, K., Streets, D.G., Hao, J.-M., 2010. Understanding of regional air pollution over China using CMAQ, part II. Process analysis and sensitivity of ozone and particulate matter to precursor emissions.

- Atmos. Environ. 44 (30), 3719–3727. <https://doi.org/10.1016/j.atmosenv.2010.03.036>.
- Liu, Y., Wang, T., 2020. Worsening urban ozone pollution in China from 2013 to 2017 – part 1: the complex and varying roles of meteorology. Atmos. Chem. Phys. 20 (11), 6305–6321. <https://doi.org/10.5194/acp-20-6305-2020>.
- Liu, Y., Shi, G., Zhan, Y., Zhou, L., Yang, F., Yang, F., Yang, F., 2021a. Characteristics of PM2.5 spatial distribution and influencing meteorological conditions in Sichuan Basin, southwestern China. Atmos. Environ. 253 <https://doi.org/10.1016/j.atmosenv.2021.118364>.
- Liu, Y., Tang, G., Huang, X., Wei, K., Wu, S., Wang, M., Wang, Y., 2021b. Unexpected deep mixing layer in the Sichuan Basin, China. Atmos. Res. 249 <https://doi.org/10.1016/j.atmosres.2020.105300>.
- Luecken, D.J., Yarwood, G., Hutzell, W.T., 2019. Multipollutant modeling of ozone, reactive nitrogen and HAPs across the continental US with CMAQ-CB6. Atmos. Environ. 194 (201), 62–72. <https://doi.org/10.1016/j.atmosenv.2018.11.060>.
- Mlawer, E.J., Taubman, S.J., Brown, P.D., Iacono, M.J., Clough, S.A., Clough, S.A., 1997. Radiative transfer for inhomogeneous atmospheres: RRTM, a validated correlated-k model for the longwave. J. Geophys. Res. Atmos. 102 (D14), 16663–16682. <https://doi.org/10.1029/97jd00237>.
- Ning, G., Wang, S., Ma, M., Ni, C., Shang, Z., Wang, J., Li, J., 2018. Characteristics of air pollution in different zones of Sichuan Basin, China. Sci. Total Environ. 612, 975–984. <https://doi.org/10.1016/j.scitotenv.2017.08.205>.
- Niu, S., Lu, C., Yu, H., Zhao, L., Liu, J., 2010. Fog research in China: An overview. Adv. Atmos. Sci. 27 (3), 639–662. <https://doi.org/10.1007/s00376-009-8174-8>.
- Noh, Y., Hong, S.-Y., Dudhia, J., 2006. A new vertical diffusion package with an explicit treatment of entrainment processes. Mon. Weather Rev. 134 (9), 2318–2341. <https://doi.org/10.1175/mwr3199.1>.
- Qiao, X., Guo, H., Tang, Y., Wang, P., Deng, W., Zhao, X., Zhang, H., 2019a. Local and regional contributions to fine particulate matter in the 18 cities of Sichuan Basin, southwestern China. Atmos. Chem. Phys. 19 (9), 5791–5803. <https://doi.org/10.5194/acp-19-5791-2019>.
- Qiao, X., Wang, P., Tang, Y., Ying, Q., Zhao, X., Deng, W., Research, A. Q., 2019b. Fine particulate matter and ozone pollution in the 18 cities of the Sichuan Basin in southwestern China: model performance and characteristics, 19 (10), 2308–2319.
- Qiao, X., Yuan, Y., Tang, Y., Ying, Q., Guo, H., Zhang, Y., Zhang, H., 2021. Revealing the origin of fine particulate matter in the Sichuan Basin from a source-oriented modeling perspective. Atmos. Environ. 244 <https://doi.org/10.1016/j.atmosenv.2020.117896>.
- Shao, T., Wang, P., Yu, W., Gao, Y., Zhu, S., Zhang, Y., Zhang, H., 2023. Drivers of alleviated PM_{2.5} and O₃ concentrations in China from 2013 to 2020. Resour. Conserv. Recycl. 197 <https://doi.org/10.1016/j.resconrec.2023.107110>.
- Shen, H., Tao, S., Chen, Y., Caias, P., Guneralp, B., Ru, M., Zhao, S., 2017. Urbanization-induced population migration has reduced ambient PM_{2.5} concentrations in China. Sci. Adv. 3 (7), e1700300 <https://doi.org/10.1126/sciadv.1700300>.
- Skamarock, W.C., Klemp, J.B., Dudhia, J., Gill, D.O., Liu, Z., Berner, J., Barker, D.M., 2019. A description of the advanced research WRF version 4, p. 145.
- Tai, A.P.K., Mickley, L.J., Jacob, D.J., 2010. Correlations between fine particulate matter (PM) and meteorological variables in the United States: implications for the sensitivity of PM to climate change. Atmos. Environ. 44 (32), 3976–3984. <https://doi.org/10.1016/j.atmosenv.2010.06.060>.
- Tao, M.H., Chen, L.F., Su, L., Tao, J.H., 2012. Satellite observation of regional haze pollution over the North China Plain. J. Geophys. Res.-Atmos. 117 (D12) <https://doi.org/10.1029/2012jd017915>.
- Tao, J., Zhang, L., Cao, J., Zhang, R., 2017. A review of current knowledge concerning PM_{2.5} chemical composition, aerosol optical properties and their relationships across China. Atmospheric Chemistry and Physics 17 (15), 9485–9518. <https://doi.org/10.5194/acp-17-9485-2017>.
- USEPA, 2022. US EPA Office of Research and Development, CMAQ (5.4). Zenodo. <https://doi.org/10.5281/zenodo.7218076>.
- Wang, L.T., Wei, Z., Yang, J., Zhang, Y., Zhang, F.F., Su, J., Zhang, Q., 2014. The 2013 severe haze over southern Hebei, China: model evaluation, source apportionment, and policy implications. Atmos. Chem. Phys. 14 (6), 3151–3173. <https://doi.org/10.5194/acp-14-3151-2014>.
- Wang, H., Tian, M., Chen, Y., Shi, G., Liu, Y., Yang, F., Cao, X., 2018a. Seasonal characteristics, formation mechanisms and source origins of PM_{2.5} in two megacities in Sichuan Basin, China. Atmos. Chem. Phys. 18 (2), 865–881. <https://doi.org/10.5194/acp-18-865-2018>.
- Wang, X., Dickinson, R.E., Su, L., Zhou, C., Wang, K., Wang, K., Wang, K., 2018b. PM_{2.5} pollution in China and how it has been exacerbated by terrain and meteorological conditions. Bull. Am. Meteorol. Soc. 99 (1), 105–119. <https://doi.org/10.1175/bams-d-16-0301.1>.
- Wang, P., Guo, H., Hu, J., Kota, S.H., Ying, Q., Zhang, H., 2019. Responses of PM(2.5) and O₃ concentrations to changes of meteorology and emissions in China. Sci. Total Environ. 662, 297–306. <https://doi.org/10.1016/j.scitotenv.2019.01.227>.
- Wang, H., Liu, Z., Wu, K., Qiu, J., Zhang, Y., Ye, B., He, M., 2022. Impact of urbanization on meteorology and air quality in Chengdu, a Basin City of southwestern China. Front. Ecol. Evol. 10 <https://doi.org/10.3389/fevo.2022.845801>.
- Wang, K., Gao, C., Wu, K., Liu, K., Wang, H., Dan, M., Tong, Q., 2023. ISAT v2.0: an integrated tool for nested-domain configurations and model-ready emission inventories for WRF-AQM. Geosci. Model Dev. 16 (7), 1961–1973. <https://doi.org/10.5194/gmd-16-1961-2023>.
- Wang, H., Qiu, J., Liu, Y., Fan, Q., Lu, X., Zhang, Y., Wang, H., 2024. MEIAT-CMAQ: a modular emission inventory allocation tool for Community Multiscale Air Quality Model. Atmos. Environ. 331 <https://doi.org/10.1016/j.atmosenv.2024.120604>.
- Wu, K., Wang, Y., Qiao, Y., Liu, Y., Wang, S., Yang, X., Lei, Y., 2022. Drivers of 2013–2020 ozone trends in the Sichuan Basin, China: impacts of meteorology and precursor emission changes. Environ. Pollut. 300, 118914 <https://doi.org/10.1016/j.envpol.2022.118914>.
- Xing, J., Mathur, R., Pleim, J., Hogrefe, C., Gan, C.M., Wong, D.C., Pouliot, G., 2015. Observations and modeling of air quality trends over 1990–2010 across the northern hemisphere: China, the United States and Europe. Atmos. Chem. Phys. 15 (5), 2723–2747. <https://doi.org/10.5194/acp-15-2723-2015>.
- Xu, L., Pye, H.O.T., He, J., Chen, Y., Murphy, B.N., Ng, L.N., 2018. Experimental and model estimates of the contributions from biogenic monoterpenes and sesquiterpenes to secondary organic aerosol in the southeastern United States. Atmos. Chem. Phys. 18 (17), 12613–12637. <https://doi.org/10.5194/acp-18-12613-2018>.
- Xu, Y., Xue, W., Lei, Y., Huang, Q., Zhao, Y., Cheng, S., Wang, J., 2020. Spatiotemporal variation in the impact of meteorological conditions on PM_{2.5} pollution in China from 2000 to 2017. Atmos. Environ. 223 <https://doi.org/10.1016/j.atmosenv.2019.117215>.
- Yang, J., Kang, S., Ji, Z., Chen, X., Yang, S., Lee, S.-Y., Chen, D., 2020. A hybrid method for PM_{2.5} source apportionment through WRF-Chem simulations and an assessment of emission-reduction measures in western China. Atmos. Res. 236 <https://doi.org/10.1016/j.atmosres.2019.104787>.
- Yu, S., Gao, W., Xiao, D., Peng, J., 2015. Observational facts regarding the joint activities of the southwest vortex and plateau vortex after its departure from the Tibetan plateau. Adv. Atmos. Sci. 33 (1), 34–46. <https://doi.org/10.1007/s00376-015-5039-1>.
- Zhang, C.-C., Xie, M., Fang, D.-X., Wang, T.-J., Wu, Z., Lu, H., Zhao, M., 2019. Synoptic weather patterns and their impacts on regional particle pollution in the city cluster of the Sichuan Basin, China. Atmos. Environ. 208, 34–47. <https://doi.org/10.1016/j.atmosenv.2019.03.033>.
- Zhang, S., Zhang, Z., Li, Y., Du, X., Qu, L., Tang, W., Meng, F., 2023. Formation processes and source contributions of ground-level ozone in urban and suburban Beijing using the WRF-CMAQ modelling system. J. Environ. Sci. (China) 127, 753–766. <https://doi.org/10.1016/j.jes.2022.06.016>.
- Zhang, Y., Liu, P., Pun, B., Seigneur, C., 2006. A comprehensive performance evaluation of MMS5-CMAQ for the summer 1999 southern oxidants study episode—part I: evaluation protocols, databases, and meteorological predictions. Atmos. Environ. 40 (26), 4825–4838. <https://doi.org/10.1016/j.atmosenv.2005.12.043>.
- Zheng, B., Tong, D., Li, M., Liu, F., Hong, C., Geng, G., Zhang, Q., 2018. Trends in China's anthropogenic emissions since 2010 as the consequence of clean air actions. Atmos. Chem. Phys. 18 (19), 14095–14111. <https://doi.org/10.5194/acp-18-14095-2018>.
- Zheng, B., Zhang, Q., Geng, G., Chen, C., Shi, Q., Cui, M., He, K., 2021. Changes in China's anthropogenic emissions and air quality during the COVID-19 pandemic in 2020. Earth System Science Data 13 (6), 2895–2907. <https://doi.org/10.5194/essd-13-2895-2021>.
- Zheng, H., Zhao, B., Wang, S., Wang, T., Ding, D., Chang, X., Wu, Y., 2019. Transition in source contributions of PM_{2.5} exposure and associated premature mortality in China during 2005–2015. Environ. Int. 132, 105111 <https://doi.org/10.1016/j.envint.2019.105111>.
- Zhou, Z., Tan, Q., Liu, H., Deng, Y., Wu, K., Lu, C., Zhou, X., 2019. Emission characteristics and high-resolution spatial and temporal distribution of pollutants from motor vehicles in Chengdu, China. Atmospheric Pollution Research 10 (3), 749–758. <https://doi.org/10.1016/j.apr.2018.12.002>.